Decarbonization of Heavy Diesel Engines: Comparative Analysis of Biodiesel and Hydrotreated Vegetable Oil (HVO) through Computational Modeling and Experimental Validation

Fábio Cordeiro de Lisboa
Danilo Almeida Machado
Guenther Carlos Krieger Filho
Universidade de São Paulo - USP
fabiolisboa@unb.br
dmachadoam@gmail.com
guenther@usp.br

ABSTRACT

The decarbonization of heavy-duty diesel transport is crucial to reducing greenhouse gas emissions. This study analyzes the replacement of fossil diesel with biodiesel and hydrotreated vegetable oil (HVO) using a computational model validated experimentally. Engine performance with pure diesel, biodiesel, HVO, and their blends were assessed using empirical and thermodynamic equations to estimate power, specific fuel consumption, and emissions. Combustion was modeled with the Wiebe equation, while quasi-dimensional and multi-zone approaches optimized performance and processing time. NOx formation was estimated via the Zeldovich mechanism and a detailed kinetic model. Experimental validation on a dynamometer and gas analyzer showed strong agreement with simulations. Results indicate an 11% power loss with biodiesel and 1% with HVO, a 28% rise in fuel consumption with biodiesel, and a 2.6% drop with HVO. B100 increased CO_2 emissions by 14%, while HVO reduced them by 5%. NOx emissions fell significantly with HVO and rose with B100. HVO proved more suitable for engines calibrated for fossil diesel.

INTRODUCTION

Biodiesel has been gaining popularity as a renewable substitute for fossil diesel due to its compatibility with current engine technologies and, generally, its lower pollutant emissions. The most used vegetable oils for biodiesel production include soybean oil, canola oil, coconut oil, and palm oil (1). Biodiesel fuels produced from different feedstock exhibit distinct effects on combustion characteristics and emissions, owing to variations in the composition of fatty acid methyl esters (FAME). The saturation level of biodiesel components also influences emission levels. Moreover, oxygen content and physicochemical properties such as viscosity and density — related to the hydrocarbon (HC) chain length — play a significant role in combustion processes (2–5).

Studies report that the use of biodiesel in diesel engines can reduce HC and CO emissions, although it is usually accompanied by power losses and increased fuel consumption (1,6). There is disagreement in the literature regarding particulate matter (PM) emissions: while some authors (7,8) associate biodiesel use with reduced soot formation due to its oxygen content (9,10), others report increases in PM, CO, and HC emissions in cycles such as the New European Driving Cycle (NEDC), attributing this behavior to the distinct physicochemical properties of biodiesel, which affect atomization and mixture formation.

In this context, several studies have sought to understand the atomization and combustion characteristics of advanced biofuels, such as methyl esters from vegetable oils and hydrotreated vegetable oil (HVO). Studies such as that of BOHL et al. (11) demonstrate that, even with similar spray areas, fuels like HVO, due to their lower density and viscosity, promote better air-fuel mixture distribution, directly impacting combustion performance. Complementarily, SHEPEL et al. (12) highlight that using blends with varying HVO and FAME ratios significantly affects emissions and thermal efficiency, with HVO standing out for generating lower NOx, HC, and particulate emissions, especially under higher loads. In contrast, blends with higher FAME content and unsaturated fatty acids tend to exhibit longer combustion durations and higher CO_2 emissions at low loads.

Additionally, computational studies have shown that the performance of biodiesel in compression ignition engines is strongly related to its molecular structure. Tan, Ng, and Gan (13) demonstrated that the hydrocarbon chain length and degree of unsaturation affect both the heat release rate and the start and end of combustion. Their results indicate that while conventional diesel offers better performance at low loads, fuels such as CME (coconut methyl ester) exhibit significant improvements at high power outputs, with lower soot emissions. The formation and transport of soot inside

the cylinder have also been investigated in studies using CFD coupled with kinetic models and deposition and transport mechanisms, revealing the role of thermophoresis and blow-by in lubricant contamination and component wear.

Given this evidence, the present study aims to deepen the understanding of how fuel molecular structure affects diesel engine performance and emissions through computational simulations using a previously validated model. The performance, specific fuel consumption, and emissions resulting from the use of mineral diesel, biodiesel, and HVO (hydrotreated vegetable oil) were analyzed. Combustion modeling was performed using the Wiebe function, coupled with quasi-dimensional and multi-zone models, aiming to optimize result accuracy and reduce computational time. NOx formation was estimated using the Zeldovich mechanism. The experimental validation, carried out on a dynamometer test bench equipped with a gas analyzer, demonstrated a high correlation with the simulated data. This study is expected to contribute to the development of renewable fuels with superior environmental and energy performance, especially under varying diesel engine load conditions.

METHODOLOGY

This study employed an integrated approach, combining computational modeling and experimental validation to investigate the influence of fuel molecular structure on the performance and emissions of compression ignition engines. The research involved fuel property characterization, combustion model implementation, engine operation simulation, and experimental validation using a diesel engine commonly used in trucks, featuring four cylinders, turbocharging, intercooling, and a 3.9L displacement volume.

The fuels considered included conventional Pure S10 diesel (B0), pure Soybean-based biodiesel (B100), and hydrotreated vegetable oil (HVO). Properties such as density, viscosity, lower heating value (LHV), oxygen content, and cetane number were obtained from the literature to ensure accurate model representation. For each case, surrogate fuels were defined — those with well-known combustion kinetics — such as methyl decanoate for biodiesel, n-hexadecane for HVO, and n-heptane for diesel, due to their ability to replicate ignition quality and combustion characteristics of the real fuels (18–21). The fuel properties used can be found in Table 1 below:

Table 1 Properties of the fuels evaluated

Property	**B0**	**B100**	**HVO**
- Carbon ($\%_{mm}$)	0.8626	0,7731	0,85
- Hydrogen ($\%_{mm}$)	0.1374	0,1188	0,15
- Oxygen ($\%_{mm}$)	0	0,1081	0
Sulfur Fraction in Fuel (%)	0,001	0,0	0,0
Lower Calorific Value (MJ/kg)	43.1	36,22	44,11
Apparent Activation Energy (kJ/mol)	22	12	40
Cetane number (-)	53.3	51,3	85
Fuel density at 323 K (kg/m^3)	810	885	820
Surface Tension Factor at 323 K (N/m)	0.028	0,0433	0,028
Dynamic Viscosity Coefficient at 323 K (Pa·s)	0.003	0,00463	0,003
Specific Heat of Vaporization (kJ/kg)	250	325	250
Thermal Capacity of Fuel (J/(kg· K))	1853	1853	2100
Fuel Molecular Mass (g/mol)	182	292,2	240
Diffusion Factor in atmospheric conditions ($\times 10^{-10}$s)	3.1	3,1	3,1
Fuel Temperature (K)	380	380	380
Saturated Vapor Pressure at low T at 480 K (bar)	0.0477	0,001	0,0477
Saturated Vapor Pressure (Pv) at T critical at 710 K (bar)	1.616	1,576	1,616

The combustion models were implemented in the AVL Cruise M with a 1D and multi-zone structure. The compression and expansion times were modeled using the polytropic ratio:

$$PV^n = \text{const} \tag{1}$$

The pressure in the cylinder was calculated from the first law of thermodynamics:

$$\frac{dQ_{comb}}{d\theta} = \frac{\gamma}{\gamma - 1} P \frac{dV}{d\theta} + \frac{1}{\gamma - 1} V \frac{dP}{d\theta} + \frac{dQ_{loss}}{d\theta} \tag{2}$$

where θ represents the angle of the crankshaft, P is the pressure, V is the volume, Q_{comb} is the heat released by combustion, and Q_{loss} represents the losses due to heat transfer. Heat transfer was modeled using Woschni's correlation:

$$h = 3.26 \cdot B^{-0.2} P^{0.8} T^{-0.55} \omega^{0.8} \tag{3}$$

with B as the cylinder diameter, P the pressure, T the gas temperature, and ω the average piston velocity.

The heat release rate (HRR) was modeled using a double Wiebe function to represent the premixed and diffusive combustion phases:

$$x_b = a\left(1 - e^{-m\left(\frac{\theta - \theta_0}{\Delta\theta}\right)^n}\right) + (1 - a)\left(1 - e^{-m_2\left(\frac{\theta - \theta_0}{\Delta\theta_2}\right)^{n_2}}\right) \tag{4}$$

Where x_b is the fraction of the mass burned, a is the fraction attributed to premixed combustion, θ_0 is the start of combustion and m, n are the shape parameters.

NOx formation was estimated using Zeldovich's extended mechanism and a reduced chemical kinetic model (Fig.1). The thermal formation of NO was modeled by (Eq. 5), as follows:

$$\frac{d[\mathrm{NO}]}{dt} = AT^{n}e^{-\frac{E_a}{RT}}[\mathrm{N_2}][\mathrm{O}] \qquad (5)$$

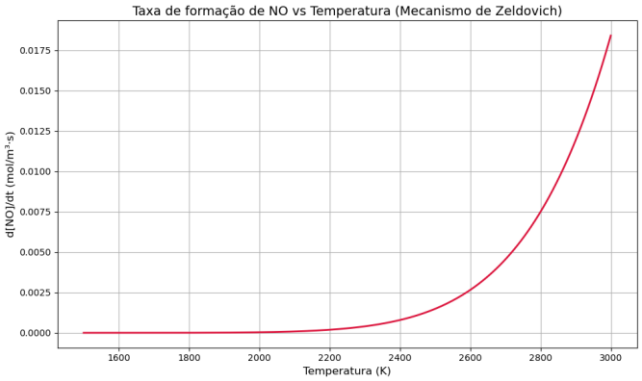

Figure 1 NO formation rate

A reduced chemical kinetic mechanism comprising 60 species and approximately 300 reactions was implemented using CHEMKIN-based libraries and subsequently converted to Cantera in Python. This enabled the simulation of ignition delay times, intermediate species formation, and post-flame reactions relevant to NO_x and soot formation processes.

Numerical simulations were performed under steady-state conditions at engine speeds of 2000 and 3000 RPM, considering load levels of 25%, 50%, 75%, and 100%. The fuel injection timing was fixed at 10° crank angle before top dead center (BTDC), and the compression ratio was maintained at 17:1 for all cases. Each fuel was subjected to identical operating conditions to enable a consistent and comparative assessment of performance and emissions. A convergence criterion was adopted, requiring pressure variation below 1% and stabilization of the heat release rate profile to ensure numerical reliability.

Experimental tests were conducted using a chassis dynamometer and an appropriately instrumented compression ignition engine. Exhaust emissions of NO_x, CO, CO_2, HC, and O_2 were quantified using a NAPRO PC Multigas analyzer, following standardized procedures [22].

This methodological approach enables a comprehensive evaluation of how variations in fuel molecular structure influence combustion dynamics and pollutant formation in compression ignition engines. The results contribute to the design and optimization of renewable fuel blends with enhanced environmental and energetic performance.

RESULTS

Figure 2 presents the experimental and simulated results for engine power, torque, and brake specific fuel consumption (bsfc) across different rotational speeds. The simulation data demonstrates a strong agreement with experimental trends, particularly for power and torque. The torque curve from the simulations closely matches the measured values, with minor deviations observed in intermediate operating conditions, indicating an adequate calibration of the model regarding mechanical performance.

Power output also exhibits good correlation, although a slight underprediction is observed near peak values. In the case of bsfc, the simulated curve (Sim_sfc) aligns well with experimental measurements, especially in the 1500–2500 RPM range. However, greater discrepancies are noted at lower speeds, where the model tends to overestimate fuel consumption.

Overall, the simulation model shows robust predictive capability, validating its applicability in assessing engine performance and energy efficiency across a wide range of operating conditions.

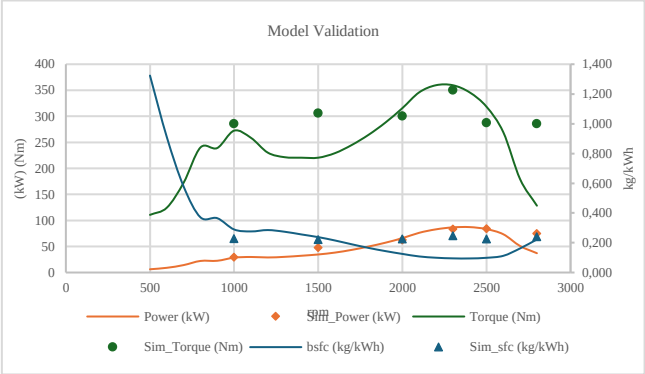

Figure 2 Comparison between measured and simulated performance data

Figure 3 presents the energy performance of B0 (pure conventional diesel), hydrotreated vegetable oil (HVO), and B100 (biodiesel) in a compression ignition engine operating at 2300 rpm. Notable differences are observed in key parameters such as effective power (P_{eng}), torque, specific fuel consumption (bsfc), and indicated thermal efficiency (η_i).

Among the tested fuels, HVO exhibited the highest performance, delivering 78.3 kW of power and 325.1 Nm of torque. These values surpass those of B0 (72.1 kW and 299.2 Nm) and B100 (65.0 kW and 269.7 Nm), highlighting the superior combustion characteristics of HVO. This is further supported by its lower sfc (0.22 kg/kWh) and higher indicated thermal efficiency (η_i = 0.42863), indicating more efficient energy conversion from chemical to mechanical work.

In contrast, B100 presented the highest sfc (0.32 kg/kWh) and the lowest power output among the tested fuels, suggesting performance limitations attributable to its physicochemical properties, such as lower volatility and oxygen content.

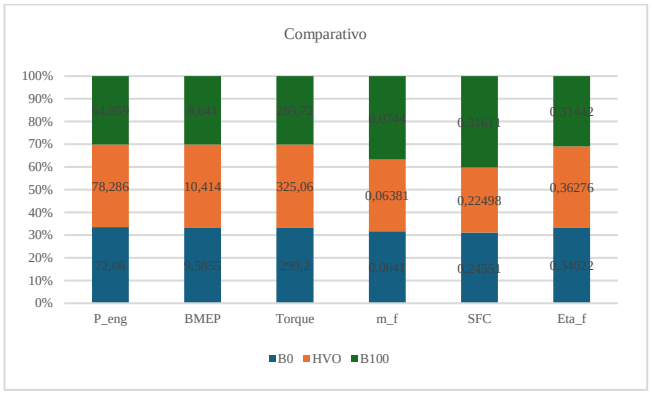

Figure 3 Energy performance 4.5L engine at 2300rpm

With respect to overall system efficiencies (Fig. 3), HVO also exhibited the highest mechanical efficiency (η_m = 0.84) and effective thermal efficiency (η_f = 0.36), reinforcing its potential as a viable substitute for fossil diesel in automotive applications. B0 showed balanced performance, with good energy conversion (η_f = 0.34) and moderate specific fuel consumption. In contrast, B100 resulted in the lowest thermal efficiency (η_f = 0.31) and mechanical efficiency (η_m = 0.82), which can be attributed to its higher viscosity and lower heating value. Nonetheless, both IMEP and BMEP values indicate that stable engine operation was maintained across all tested fuels. These findings underscore the suitability of HVO as an efficient and low-carbon alternative fuel, if fuel injection and air management systems are appropriately calibrated.

Figure 4 presents key thermodynamic and injection parameters for HVO and B100, highlighting significant differences in their combustion behavior under Diesel cycle operation. HVO produced the highest peak pressure (110.9 bar) and maximum in-cylinder temperature (2064.3 K), along with a steeper pressure rise rate (3.9 bar/°CA), reflecting a more rapid and intense combustion process. This behavior is further evidenced by the greater combustion intensity (Ring_Intn = 2.1) and higher peak internal force (F_{max} = 9177.7 N), which may affect component durability.

In comparison, EN590 exhibited a less aggressive combustion profile, characterized by more effective fuel atomization (Sauter mean diameter d_{32} = 11.6 µm) and shorter ignition delay. B100 demonstrated intermediate behavior, consistent with its higher viscosity and longer ignition delay.

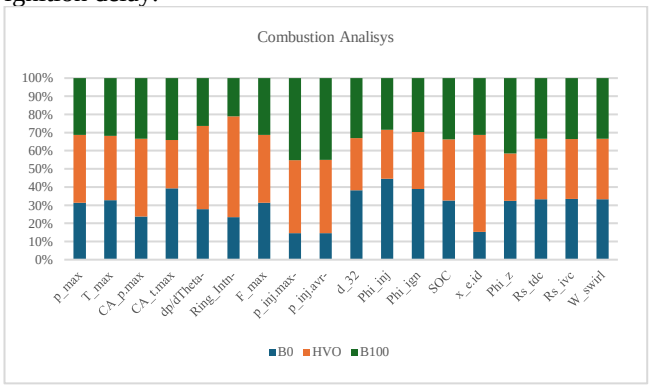

Figure 4 Combustion parameters

Regarding injection parameters, both HVO and B100 required significantly higher injection pressures—averaging 2463.7 bar and 2748.5 bar, respectively—compared to 890.6 bar for EN590. This disparity stems from the distinct physicochemical properties of the biofuels, which demand more energy for proper atomization. Despite these differences, the start of combustion (SOC) remained relatively consistent across fuels, occurring between 7.9°CA and 8.1°CA.

These results indicate that biofuels, particularly HVO, can enhance thermal performance; however, their successful application depends on precise fuel injection system calibration and the mechanical robustness of engine components due to elevated combustion intensities. The findings contribute to a deeper understanding of alternative fuel behavior in compression ignition engines and support the development of optimized control strategies for renewable fuel integration.

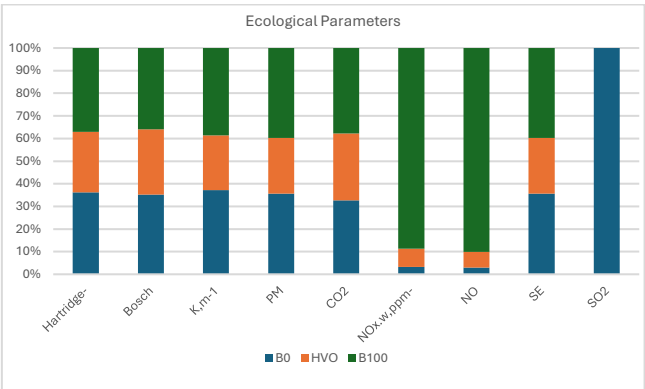

Figure 5 Ecological parameters

A comparative analysis of B0, HVO, and B100 fuels reveals significant differences in emissions (Fig. 5) and performance parameters (Fig. 3). B0 exhibited intermediate opacity values (Hartridge: 57.4; Bosch: 4.3) and particulate matter emissions (PM: 2.0 mg/m³), with moderate CO_2 levels (784.4 ppm) and the lowest NO_x (0.0018 ppm) and NO (8.92×10^{-6} ppm) emissions.

HVO stood out for its lower opacity indices (Hartridge: 42.5; Bosch: 3.5), PM emissions (1.3 mg/m³), CO_2 (708.3 ppm), smoke emission index (SE: 2.8), and zero SO_2 emissions, indicating environmental superiority over the other fuels. Conversely, B100 showed the highest values for opacity (Hartridge: 58.8), PM (2.1 mg/m³), CO_2 (905.1 ppm), NO_x (0.0475 ppm), and NO (2.67×10^{-4} ppm), suggesting a higher environmental impact, although no SO_2 emissions were detected.

These results highlight that although B100 is a renewable fuel, its environmental performance regarding emissions may be inferior to alternatives such as HVO, particularly in controlling NO_x and particulate matter.

CONCLUSION

This study aimed to evaluate the performance and energy efficiency of different fuels (B0, HVO, and B100) in a Diesel engine using a validated simulation model to analyze power, torque, and specific fuel consumption

parameters. The model validation showed good accuracy in predicting engine mechanical performance, with minor variations observed in torque and power across mid-range operating conditions, indicating proper calibration. The model also demonstrated adequate predictive capability for SFC, despite slight overestimations at low engine speeds.

The comparative analysis revealed that HVO provided the best overall performance, delivering higher power, torque, thermal efficiency, and lower SFC, making it a strong candidate for the partial decarbonization of the transportation sector. Although B100 is renewable, it exhibited the lowest performance, with increased SFC and reduced power, primarily due to its physicochemical properties, such as higher viscosity and lower calorific value. Diesel B0 displayed balanced characteristics, with intermediate energy conversion efficiency.

Furthermore, thermodynamic and injection data showed distinct combustion behaviors among the fuels. HVO exhibited more intense combustion, which could increase mechanical stress, necessitating careful injection calibration. B100 required elevated injection pressures due to its viscosity, though combustion phasing was similar across all fuels.

In terms of emissions, HVO again proved to be the most environmentally favorable option, with reduced opacity, PM, and CO_2 emissions. In contrast, B100 contributed more significantly to NO_x and PM emissions. These insights are essential for developing more robust and efficient control strategies aimed at maximizing engine performance while minimizing environmental impact using alternative fuels in Diesel engines.

BIBLIOGRAPHY

1. Demirbas A. Progress and recent trends in biodiesel fuels. Energy Convers Manag. 2009; 50(1):14–34.
2. Cardone M, Prati MV, Rocco V, Seggiani M, Senatore A, Vitolo S. Brassica carinata as an alternative oil crop for the production of biodiesel in Italy: engine performance and regulated and unregulated exhaust emissions. Environ Sci Technol. 2002; 36(21):4656–62.
3. Di Y, Cheung CS, Huang Z. Experimental investigation on regulated and unregulated emissions of a diesel engine fueled with ultra-low sulfur diesel fuel blended with biodiesel from waste cooking oil. Science of the total environment. 2009; 407(2):835–46.
4. Hossain AK, Davies PA. Plant oils as fuels for compression ignition engines: A technical review and life-cycle analysis. Renew Energy. 2010; 35(1):1–13.
5. Janaun J, Ellis N. Perspectives on biodiesel as a sustainable fuel. Renewable and Sustainable Energy Reviews. 2010; 14(4):1312–20.
6. Xue J, Grift TE, Hansen AC. Effect of biodiesel on engine performances and emissions. Renewable and Sustainable energy reviews. 2011; 15(2):1098–116.
7. Agarwal AK, Bijwe J, Das LM. Effect of biodiesel utilization of wear of vital parts in compression ignition engine. J Eng Gas Power Turbines. 2003; 125(2):604–11.
8. Reksowardojo IK, Dung NN, Tuyen TQ, Sopheak R, Brodjonegoro TP, Soerwidjaja TH, et al. The comparison the effect of biodiesel fuel from palm oil and physic nut oil (Jatropha curcas) on an direct injection (DI) diesel engine. In: Proceedings of FISITA 2006 conference in Yokohama, Japan. 2006.
9. Fontaras G, Karavalakis G, Kousoulidou M, Tzamkiozis T, Ntziachristos L, Bakeas E, et al. Effects of biodiesel on passenger car fuel consumption, regulated and non-regulated pollutant emissions over legislated and real-world driving cycles. Fuel. 2009; 88(9):1608–17.
10. Ng JH, Ng HK, Gan S. Advances in biodiesel fuel for application in compression ignition engines. Clean Technology Environ Policy. 2010; 12:459–93.
11. Bohl T, Tian G, Smallbone A, Roskilly AP. Macroscopic spray characteristics of next-generation bio-derived diesel fuels in comparison to mineral diesel. Appl Energy. January 2017; 186:562–73.
12. Shepel O, Matijošius J, Rimkus A, Duda K, Mikulski M. Research of Parameters of a Compression Ignition Engine Using Various Fuel Mixtures of Hydrotreated Vegetable Oil (HVO) and Fatty Acid Esters (FAE). Energies (Basel). May 25, 2021; 14(11):3077.
13. Tan SM, Ng HK, Gan S. Numerical Studies of In-Cylinder Combustion and Soot Emission Characteristics of Biodiesel Fuels from Different Feedstock. Journal of Advanced Research in Fluid Mechanics and Thermal Sciences. April 24, 2020; 70(1):46–61.
14. Ray SC, Safiullah, Naito S, Andersson M, Nishida K, Ogata Y. Characterization of diesel spray with novel high-speed laser absorption scattering technique under diesel engine-like condition. Int J Heat Mass Transf. 2024 May;222:125103.
15. Ayad SMME, Zanella IZ, de Brito CHG, Torres ER, Belchior CRP, de Oliveira PL, et al. Study on the effects of micro-addition of hydrogen in diesel combustion in an optically accessible engine. Int J Hydrogen Energy. July 2024; 75:363–87.
16. Pal MK, Bhagwat A. Modification of a multihole injector to a single-hole injector and spray characteristics of the modified injector by two different imaging techniques. Journal of Flow Visualization and Image Processing. 2023; 30(4):117–35.
17. Tinchon A, Foucher F, Doradoux L. Hydrogen Jet Characterization of an Internal Combustion Engine Injector Using Schlieren Imaging. In 2023.
18. Herbinet O, Pitz WJ, Westbrook CK. Detailed chemical kinetic oxidation mechanism for a biodiesel surrogate. Combust Flame. August 2008; 154(3):507–28.

19. Herbinet O, Pitz WJ, Westbrook CK. Detailed chemical kinetic mechanism for the oxidation of biodiesel fuels blend surrogate. Combust Flame. May 2010; 157(5):893–908.
20. Pei Y, Mehl M, Liu W, Lu T, Pitz WJ, Som S. A multicomponent blend as a diesel fuel surrogate for compression ignition engine applications. J Eng Gas Turbine Power. 2015; 137(11):111502.
21. Curran HJ, Gaffuri P, Pitz WJ, Westbrook CK. A comprehensive modeling study of n-heptane oxidation. Combust Flame. 1998; 114(1–2):149–77.
22. Lisboa F, Wohlgemuth J, Lima de Oliveira N. Assessment of Emissions and Fuel Consumption in Heavy Trucks: Implications of Biodiesel Blending in Brazil's Fleet. In: Procceedings of the 20th Brazilian Congress of Thermal Sciences and Engineering. ABCM; 2024.